The authors and co-workers are currently extending the procedure to manage cooperation between constellations of satellites.[5]

Conclusions

We have outlined a scheme for sequencing of tasks on a microspacecraft platform. The scheme is easily implemented by virtue of its computational simplicity. Moreover, the strategy is derived from optimal control theory. Action selection with the cue-deficit algorithm is seen to perform well on our microsatellite simulation and is demonstrably robust to significant failures of the satellite solar array. Our work has also demonstrated robustness to failures of payload, transmitters, and injection into nonoptimum orbits (such as elliptical transfer orbits, rather than the mission orbit) although these results are not shown here for brevity.

Acknowledgment

This work was partially supported by a Grant from the Leverhulme Trust.

References

[1]Creasey, R., "Implementing Spacecraft Autonomy Using Discrete Control Theory," *Space Technology*, Vol. 16, No. 2, 1996, pp. 109–116.

[2]Horvath, J., "Spacecraft Autonomy Issues: Present and Future," *Journal of the British Interplanetary Society*, Vol. 49, No. 6, 1996, pp. 215, 216.

[3]Spier, E., and McFarland, D., "Finer-Grained Motivational Model of Behaviour Sequencing," *4th International Conference on Simulation of Adaptive Behaviour*, MIT Press, Cambridge, MA, 1996, pp. 255–263.

[4]McFarland, D., and Spier, E., "Basic Cycles, Utility and Opportunism in Self-Sufficient Robots," *Robotics and Autonomous Systems*, Vol. 20, Nos. 2–4, 1997, pp. 179–190.

[5]Radice, G., Gillies, E., Johnstone, G., and McInnes, C., "Autonomous Action Selection for Micro-Satellite Constellations," International Astronautical Foundation, Paper ST-98-W.1.05, 1998.

Effects of Planar Thrust Misalignments on Rigid Body Motion

Daniel Levy de F. Rodrigues* and
Marcelo Lopes de O. e Souza†
National Institute for Space Research,
12227-010 São José dos Campos, Brazil

Introduction

SPACE vehicles are frequently designed to have propulsive systems capable of generating longitudinal forces with the thrust axis passing through the c.m. of the vehicle. However, in many practical cases this does not occur, and a disturbance torque appears. The misalignments can be angular or linear. Such misalignments usually have low magnitude and are mainly caused by the structural design of the vehicle, vibrations, the motion of movable parts (especially liquids), and displacements of the c.m. caused by fuel consumption.[1] Schwende and Strobl[2] mention as reasonable an angular misalignment $\delta < 0.002$ rad for a typical apogee motor.

In the case of orbital transfers, the misalignment torque—even with small magnitude—is very important because it alters the force orientation with respect to the specified strategy and, as a consequence, produces an error with respect to the desired final orbit, thus generating the necessity of implementing a fast and precise active attitude control during the orbital transfer. Longuski et al.[3] present a control proposal that eliminates the damage caused by this misalignment during propulsive maneuvers. Their proposal consists of splitting it in two parts, intercalated by a time interval without propulsion. The spin stabilization is a strategy that has also shown very much use in apogee motors, by canceling the torque of the transverse misalignment.

In this work we intend to verify analytically the effects of planar thrust misalignments on rigid body motion, supposing the absence of a fast and precise active attitude control during the propulsion. A numerical example illustrates the situation for a hypothetical vehicle. Details are in Chap. 5 of Rodrigues.[4]

Simplified Analytical Study

Consider a model constituted by a rigid and constant-mass vehicle subject only to a unique force with a constant orientation with respect to the vehicle's principal inertia axes and with its application axis not intercepting the c.m. (Fig. 1). In this way, the trajectory described by the c.m. remains in the plane that contains this force and the c.m. Thus, we can choose a reference system $OXYZ$ whose plane XY contains the referred trajectory.

The equations of motion of the attitude and of the c.m. motion with respect to $OXYZ$ can be obtained as

$$I\ddot{\theta}(t) = F\varepsilon \qquad \text{where} \qquad \varepsilon = h\sin\delta + \nu\cos\delta \tag{1}$$

$$m\ddot{\boldsymbol{R}}(t) = \boldsymbol{F}(t) \tag{2}$$

where m is the body mass (supposed constant), $\boldsymbol{R}$ is the c.m. position vector with respect to the inertial reference system $OXYZ$, $\boldsymbol{F}$ is the resulting force written in terms of the $OXYZ$ vectors, h is the longitudinal distance of the ideal thrust position to the c.m., I is the inertia moment with respect to the rotation axis Z, θ is the attitude angle, ν and δ are the linear and the angular misalignments of the thrust vector, and t is the time. From Eq. (1) we get

$$\dot{\theta}(t) = (F\varepsilon/I)t + \dot{\theta}(0) \tag{3}$$

$$\theta(t) = (F\varepsilon/2I)t^2 + \dot{\theta}(0)t + \theta(0) \tag{4}$$

To avoid some mathematical difficulties, we consider zero initial conditions: $R(0) = 0$, $\dot{R}(0) = 0$, $\theta(0) = 0$, and $\dot{\theta}(0) = 0$. For the components of the c.m. position vector $X(t)$ and $Y(t)$, Eq. (2) becomes

$$m\ddot{X}(t) = F\sin[(F\varepsilon/2I)t^2 - \delta] \tag{5}$$

$$m\ddot{Y}(t) = F\cos[(F\varepsilon/2I)t^2 - \delta] \tag{6}$$

Approximate Analytical Solution

It is possible to obtain approximate solutions to Eqs. (5) and (6) for t near zero and for t growing without bound. Consider initially the case where $t \to 0$. In this case the relations $\cos\theta(t) \cong 1$ and $\sin\theta(t) \cong \theta(t)$ hold. Normally δ is very small, thus we can write $\cos\delta \cong 1$ and $\sin\delta \cong \delta$. Then Eqs. (5) and (6) can be rewritten as

$$m\ddot{X}(t) \cong (F^2\varepsilon/2I)t^2 - F\delta \tag{7}$$

$$m\ddot{Y}(t) \cong F \tag{8}$$

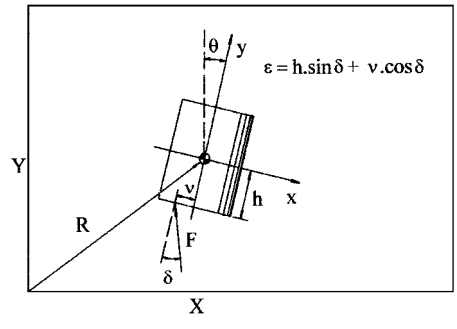

Fig. 1 Linear and angular misalignments of a simplified system in planar motion.

Received 2 November 1998; revision received 1 April 1999; accepted for publication 12 May 1999.

*Corresponding Researcher, Division of Space Mechanics and Control-DMC, INPE, Av. dos Astronautas, 1758-CP 515.

†Senior Researcher, Division of Space Mechanics and Control-DMC, INPE, Av. dos Astronautas, 1758-CP 515; marcelo@dem.inpe.br.

Equations (7) and (8) are easily integrable and give

$$\dot{X}_0(t) \cong (F^2\varepsilon/6mI)t^3 - (F\delta/m)t \tag{9}$$

$$\dot{Y}_0(t) \cong (F/m)t \tag{10}$$

$$X_0(t) \cong (F^2\varepsilon/24mI)t^4 - (F\delta/2m)t^2 \tag{11}$$

$$Y_0(t) \cong (F/2m)t^2 \tag{12}$$

where the subscript 0 indicates $t \to 0$. The powers of t in Eqs. (9–12) show that the motion degenerates quickly.

By eliminating the time between Eqs. (9) and (10) and between Eqs. (11) and (12), we get

$$\dot{X}_0(t) \cong (m^2\varepsilon/6FI)\dot{Y}_0^3(t) - \delta\dot{Y}_0(t) \tag{13}$$

$$X_0(t) \cong (m\varepsilon/6I)Y_0^2(t) - \delta Y_0(t) \tag{14}$$

This model is the simplified case of a vehicle under a propulsive system with a misalignment torque. The ideal case would be without misalignments, and, then, the vehicle c.m. trajectory would ideally be on the Y axis. Because of the presence of the misalignments, this trajectory degenerates, initially in the parabola described by Eq. (14).

Equations (9–14) describe the behavior of the body c.m. for t close to zero. In the first instants of the propulsion, the effects of the misalignments are small, as shown by Eqs. (10) and (12), that is, the component of the c.m. motion along the longitudinal axis Y follows a linear path. But the c.m. motion quickly assumes a parabolic behavior described by Eq. (14).

To obtain the c.m. behavior for very high values of t, we can integrate Eqs. (5) and (6) from 0 to $+\infty$:

$$m\int_{t=0}^{t\to\infty} \ddot{X}(t)\,\mathrm{d}t = F\int_{t=0}^{t\to\infty} \sin\left(\frac{F\varepsilon}{2I}t^2 - \delta\right)\mathrm{d}t \tag{15}$$

$$m\int_{t=0}^{t\to\infty} \ddot{Y}(t)\,\mathrm{d}t = F\int_{t=0}^{t\to\infty} \cos\left(\frac{F\varepsilon}{2I}t^2 - \delta\right)\mathrm{d}t \tag{16}$$

By formula 1, paragraph 3.691, p. 395, Sec. 3.69–3.71 of Ref. 5, we get

$$\dot{X}_\infty = \frac{\cos\delta - \sin\delta}{2m}\sqrt{\frac{\pi FI}{\varepsilon}} \tag{17}$$

$$\dot{Y}_\infty = \frac{\cos\delta + \sin\delta}{2m}\sqrt{\frac{\pi FI}{\varepsilon}} \tag{18}$$

$$X_\infty = \frac{\cos\delta - \sin\delta}{2m}\sqrt{\frac{\pi FI}{\varepsilon}}t + k_x \tag{19}$$

$$Y_\infty = \frac{\cos\delta + \sin\delta}{2m}\sqrt{\frac{\pi FI}{\varepsilon}}t + k_y \tag{20}$$

where the subscript ∞ indicates $t \to +\infty$.

Equations (17) and (18) show that for $t \to +\infty$ the c.m. velocity becomes constant despite there being a nonzero instantaneous force acting on the body, which is explained by the fact that when t becomes very large the angular velocity is so high that it almost instantaneously occupies successive opposite angular positions, canceling the linear effects of the acting force. A fast and precise attitude control would be required to avoid this.

By eliminating t between Eqs. (17) and (18) and between Eqs. (19) and (20), we get

$$\dot{Y}_\infty = \frac{\cos\delta + \sin\delta}{\cos\delta - \sin\delta}\dot{X}_\infty \tag{21}$$

$$Y_\infty = \frac{\cos\delta + \sin\delta}{\cos\delta - \sin\delta}X_\infty + k \tag{22}$$

In the ideal case (ν and $\delta = 0$) the trajectory should describe a straight line along the Y axis with speed growing linearly with time. In the real case (ν and $\delta \neq 0$) the trajectory becomes straight but not necessarily along the Y axis and with constant speed, as shown by Eqs. (17) and (18). If $\delta = \pi/4$, then the c.m. trajectory returns to have only the Y-axis component.

The c.m. trajectory was determined only for the situations described ($t \to 0$ and $t \to +\infty$), but its intermediate behavior remains unknown. Some idea of this behavior can be obtained by examining Eqs. (5) and (6). These equations show that $\dot{X}(t)$ and $\dot{Y}(t)$ present oscillatory behavior, with maximum and minimum points given by $\ddot{X}(t)$ and $\ddot{Y}(t) = 0$. Equations (17) and (18) show that the velocity components converge to constant values; therefore, the c.m. velocity must be damped oscillatory. Consequently, the c.m. trajectory for the intermediate situation should also be oscillatory.

Determining the value of t for which $\dot{Y}(t)$ reaches its maximum value is interesting. This value—denoted here by t^*—is important because it indicates that if the propulsion continues the trajectory degradation will be more and more accentuated. Thus, t^* can be understood as an upper bound to the thrust duration t_{on} of the propulsion system for a slightly degenerate c.m. trajectory. From Eq. (6) for $\dot{Y}(t)$ to be maximum t should be

$$t^* = \sqrt{\frac{I(k\pi + 2\delta)}{F\varepsilon}} \tag{23}$$

with $k = 1, 3, 5, \ldots$ and the first maximum occurring for $k = 1$. Approximating Eq. (6) by

$$m\ddot{Y}(t) \cong F\left\{1 - \frac{[(F\varepsilon/2I)t^2 - \delta]^2}{2!} + \frac{[(F\varepsilon/2I)t^2 - \delta]^4}{4!}\right\} \tag{24}$$

the value of $\dot{Y}(t^*)$, denoted by $\dot{Y}^*$, is approximated by

$$\dot{Y}^* \cong \frac{F\sqrt{I(\pi + 2\delta)/F\varepsilon}}{m}\left[1 - \frac{\pi^2}{40} + \frac{\pi^4}{3460} + \left(\frac{1}{15} - \frac{\pi^2}{1512}\right)\pi\delta + \left(\frac{\pi^2}{630} - \frac{4}{15}\right)\delta^2 - \frac{4}{945}\pi\delta^3 + \frac{16}{945}\delta^4\right] \tag{25}$$

Note that the attitude angle for this situation depends on F, ε, and I, and it will always be given by

$$\theta^* \cong (\pi/2)k + \delta \tag{26}$$

For the first maximum and for $\delta = 0$, it happens that $\theta^* = \pi/2$. This result is an extreme θ upper bound.[4]

Numerical Example

Consider the hypothetical situation where we have a straight cylindrical body with radius $r = 1$ m, height $H = 2h = 3$ m, with a force $F = 10$ N, applied perpendicularly to the base, and $\nu = 0.01$ m, $\delta = 0$ rad, $\varepsilon = 0.01$ m, $m = 5$ kg, $I = 5$ kg · m^2, $R(0) = 0$ m, $\dot{R}(0) = 0$ m/s, $\theta(0) = 0$ rad, and $\dot{\theta}(0) = 0$ rad/s.

Figures 2–4 show the simulation results for the example in question. From Fig. 2 we can observe that the c.m. velocity components have damped oscillatory behavior whose values converge to the

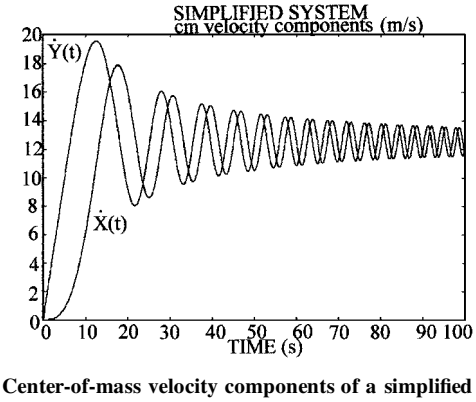

Fig. 2 Center-of-mass velocity components of a simplified system in planar motion as a function of time.

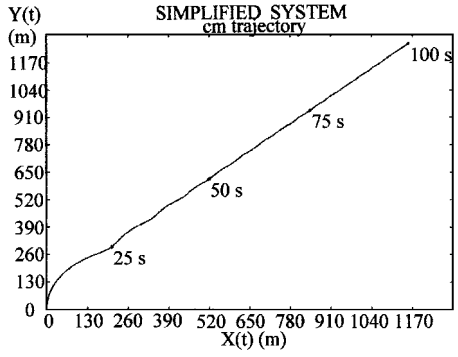

Fig. 3 Center-of-mass trajectory of a simplified system in planar motion.

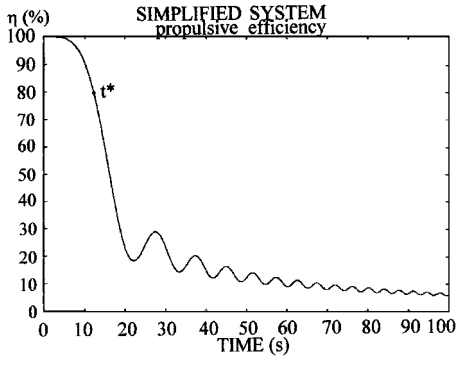

Fig. 4 Propulsive efficiency of a simplified system in planar motion.

interval of 12–14 m/s. From Eqs. (17) and (18) we get the convergence values $\dot{X}_\infty = \dot{Y}_\infty = 12.53$ m/s. The values t^* and $\dot{Y}^*$ for this example, obtained from Eqs. (23) and (25), are 12.53 s and 19.59 m/s, respectively. The actual value for $\dot{Y}^*$ is 19.55 m/s, indicating a relative error in the analytic model less than 0.5% (for this example). The ideal value of $\dot{Y}^*$, given by $(F/m)t^*$, is 25.07 m/s. Thus, the application of the force during t^* s ensures a propulsive efficiency, equal to the relation of $\dot{Y}^*$ and $(F/m)t^*$, greater than 77% in this case.

From Fig. 3 we can check that the approximate analytical solution agrees with the real solution for small t. The parabolic behavior of the c.m. trajectory described by Eq. (14) is clearly evident for small t. From Fig. 3 we also note that for large t the c.m. trajectory approaches the straight line described by Eqs. (19), (20), and (22). When $\varepsilon = 0$, the c.m. describes a straight trajectory in the Y direction, which in fact occurs in the first instants. The $\varepsilon \neq 0$ deviates this trajectory (the greater the value of ε then the faster the deviation) substantially.

From Fig. 4 we note that the propulsive efficiency η decreases monotonically with time until $\dot{Y}(t)$ reaches its first relative minimum, with $k = 3$ in Eq. (23).

Despite the numerical example being specific, Figs. 2–4 show the general behavior of the c.m. perturbations of a body subjected to the misalignment torque $F \cdot \varepsilon \cdot \hat{e}_z$. In practice, we should avoid them by reducing ε, choosing parameters that increase t^*, thrusting during $t_{on} \ll t^*$, and by using a fast and precise attitude control.

Conclusions

This Note presented an analytical study of the effects of planar thrust misalignments on rigid body motion. Using some simplifications, we showed how the c.m. behaves in the absence of attitude control. We showed that 1) the c.m. motion degenerates quickly into an initial parabolic trajectory, 2) the thrust duration t_{on} should be much smaller than an upper bound t^*, and 3) the propulsive efficiency η falls quickly if t_{on} becomes comparable to t^*.

References

[1]Tandon, G. K., "Modeling Torques due to Orbit Maneuvers," *Astrophysics and Space Science Library*, Vol. 733, 1988, pp. 580–583.

[2]Schwende, M. A., and Strobl, H., "Bi-Propellant Propulsion Systems for Spacecraft Injection and Control," edited by C. Rowley and B. Battrick, *Attitude and Orbit Control Systems Proceedings*, European Space Agency, ESA SP-128, Paris, 1977, pp. 405–412.

[3]Longuski, J. M., Kia, T., and Breckenridge, W. G., "Annihilation of Angular Momentum Bias During Thrusting and Spinning-Up Maneuvers," *The Journal of the Astronautical Sciences*, Vol. 37, No. 4, 1989, pp. 433–450.

[4]Rodrigues, D. L. F., "Dynamic Analysis of Orbital Transfers," M.S. Thesis, Dept. of Space Mechanics and Control, National Inst. for Space Research, INPE-5352-TDI/461, São José dos Campos, Brazil, Oct. 1991.

[5]Gradshteyn, I. S., and Ryzhik, I. M., *Table of Integrals, Series and Products*, Academic International Press, New York, 1980, p. 395.

Generalized Canonical Systems Applications to Optimal Trajectory Analysis

Sandro da Silva Fernandes*
Instituto Tecnológico de Aeronáutica, 12228-900 São José dos Campos, Brazil

Introduction

THE coast-arc problem[1] that defines the optimal trajectory of a constant exhaust velocity space vehicle is described by a special class of systems of differential equations, termed generalized canonical systems.[2] Such systems have intrinsic properties concerning the Mathieu transformations defined by the general solution of the system of differential equations governed by the integrable kernel of the Hamiltonian function. By using these properties, integration of the system of differential equations describing the coast arc in a Newtonian central force field is performed. As will be shown, in contrast with other methods involving numerous integrations,[3,4] the generalized canonical approach requires the evaluation of only one integral, closely related to Kepler's classic equation. A complete closed-form solution will be obtained for elliptic, circular, parabolic and hyperbolic motions.

The coast-arc problem will be formulated as proposed by Powers and Tapley[5] through a two-dimensional formulation of the equations of motion. The three-dimensional case, considering a different set of state variables and orbital elements,[6,7] was previously discussed.

Coast-Arc Problem

For completeness, previous results about the coast-arc problem are presented.[6] Let us consider the motion of a space vehicle $\mathcal{M}$ in a Newtonian central force field during a coasting period. In a two-dimensional formulation,[5] the well-known equations of motion in polar coordinates are:

$$\frac{dr}{dt} = u, \qquad \frac{du}{dt} = \frac{v^2}{r} - \frac{\mu}{r^2}, \qquad \frac{dv}{dt} = -\frac{uv}{r}, \qquad \frac{d\theta}{dt} = \frac{v}{r} \quad (1)$$

where r is the radial distance from the center of attraction O; u and v are the radial and circumferential components of the velocity, respectively; θ is the polar angle, measured from any convenient reference line through the center of attraction; and μ is the gravitational parameter. The adjoint variables associated with the state variables (r, u, v, and θ) will be denoted by (π_r, π_u, π_v, and π_θ). The coast-arc problem is then described by the following Hamiltonian function:

$$H = u\pi_r + (v^2/r - \mu/r^2)\pi_u - (uv/r)\pi_v + (v/r)\pi_\theta \quad (2)$$

Received 19 August 1998; revision received 18 May 1999; accepted for publication 26 May 1999.

*Associate Professor, Departamento de Matemática; sandro@ief.ita.cta.br.